

POST-WELD INDUCTION HEATING PROVIDES CONTROLLED COOLING OF MSS WELDS

The ductility of annealed Type 410 martensitic stainless steel (MSS) is improved by post-weld induction heating of the heat affected zone immediately following weld pool solidification. Maximum strain at fracture is increased with a corresponding decrease in ultimate tensile strength compared with as-welded specimens.

Daniel S. Codd
KVA Inc.
Escondido, Calif.

Many welded assemblies made of high strength alloys require post-weld mechanical forming operations, which creates complications when using high strength steels (HSS), whose chemical compositions can result in fully martensitic, brittle as-welded microstructures. Martensitic stainless steels (MSS) are a particular class of HSS susceptible to high fusion and heat-affected zone (HAZ) hardness after welding.

Martensitic stainless steels contain between 10.5 to 18% chromium and sufficient carbon to make them hardenable by heat treatment. Historical applications of MSS include cutlery, springs, valves, shafts, ball bearings, turbine equipment and petrochemical equipment. The steels are amenable to a quench-and-temper (Q+T) heat treatment to produce high strength and hardness. The higher carbon content of the martensitic grades results in an austenite-to-martensite transformation upon rapid cooling. MSS are considered to be air-hardenable, as all but the thickest sections fully harden during air-quenching from the austenitizing temperature to room temperature.

The thermal cycle of heating and rapid cooling that occurs within the fusion and HAZ during welding is equivalent to a rapid air-cooling quench cycle. As a result, the martensitic weld structure produced is ex-

tremely brittle in the untempered condition. Regardless of the prior condition of the steel (annealed, hardened, or hardened and tempered), welding produces a hardened martensitic fusion zone and HAZ (Fig. 1), which makes martensitic stainless steels difficult to weld^[1].

However, this material is ideally suited for structural components and assemblies, satisfying the requirements of high strength, toughness, and corrosion resistance, with ease of forming in the annealed state. Although most assemblies fabricated from these alloys would undergo a final homogenizing solution heat-treatment hardening cycle, great benefits could be realized if the as-welded brittleness could be reduced. This would make secondary processes on weldments, such as cold working, bending, flanging, and hydroforming (as in the case of seam-welded tubing) easier.

One method to reduce weld hardness is to add filler material to modify the final metallurgy to reduce the percentage of hard, brittle components such as martensite^[2]. Another approach is to heat treat the welded part during or after welding. From a production point of view, heat treatment during production is preferred to avoid costly pre or post treatment^[3].

Typical off-line methods of controlling weld and HAZ hardness include secondary post-weld heat treatments (PWHT) such as process annealing. Preheating methods can be used to slow the rate of cooling, thereby reducing the percentage of martensite formed. Unfortunately, these methods are neither cost nor time effective for high production levels associated with modern manufacturing methods. On the other hand, induction heating is an efficient way to heat treat steel parts^[4]. The simple in-line induction weld cooling control and PWHT method discussed in this article appreciably increases weld and HAZ ductility without increasing process time.

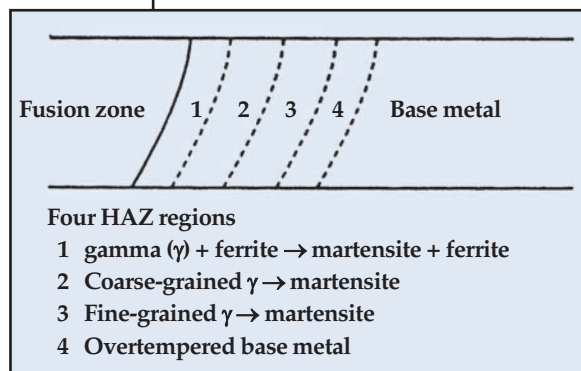


Fig. 1 — Four HAZ regions in a martensitic stainless steel weld^[1].

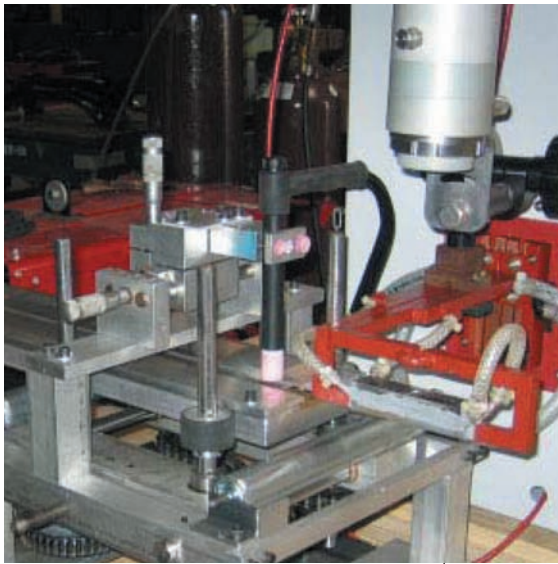


Fig. 2 — Seam weld/cooling-control test apparatus.

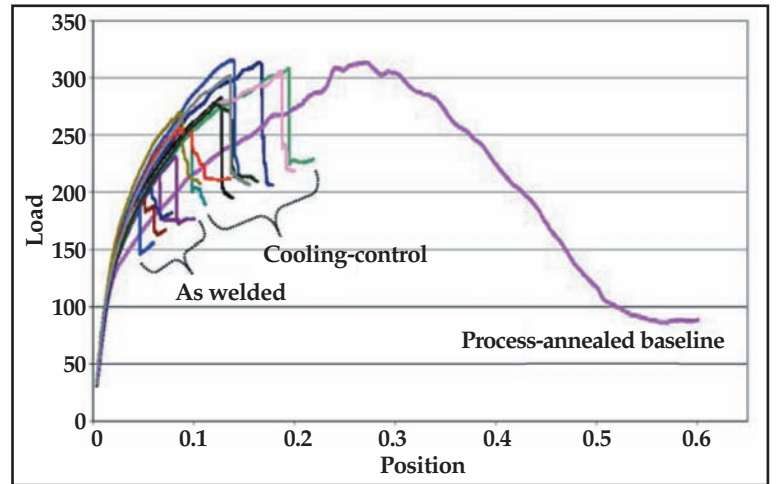


Fig. 5 — Comparison of 3-point longitudinal face-bend test load-position data for various process conditions. Modified ASTM E190 guided bend test for ductility of welds. Bend Radius = $2t$; $t = 1$ mm.

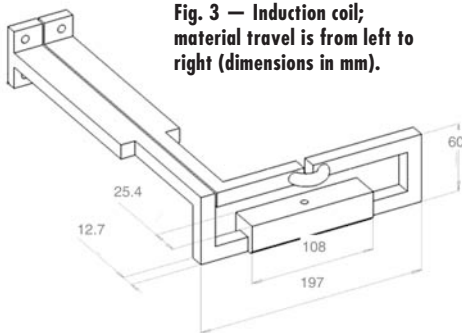


Fig. 3 — Induction coil; material travel is from left to right (dimensions in mm).

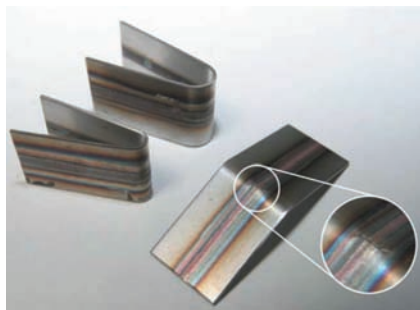


Fig. 4 — Typical ASTM E190 guided bend-test weld ductility specimens. From left: $2t$ bend radius-full bend; $4t$ bend radius-full bend; $4t$ bend radius-failure.

Experimental Procedure

The material used in this study was Type 410 martensitic stainless steel (UNS41000, SAE 51410) with a nominal chemical composition of 0.15% max C and 11.5-13.5% Cr. Chemical composition of the actual samples is shown in Table 1. Stainless sheet test strips (0.5, 1, and 2 mm thick and 1,500 mm) were butt welded in the annealed condition using gas tungsten arc welding (GTAW) in a linear seam welding test fixture (Fig. 2). Test coupons were taken from the central, steady-state portion of the weld.

A special one-sided linear induction coil (Fig. 3) was implemented downstream of the GTAW torch to control the cooling profile of the weld seam. The coil incorporated a ferrite concentrator to focus the high frequency energy into a linear pattern directed onto the weld seam. A split coil design with a novel through-coil sight bore allowed for direct surface temperature measurements using a noncontact infrared pyrometer.

Optimal baseline GTAW settings were maintained throughout the controlled-cooling trials to isolate the effects of the secondary heat source on weld quality. Direct surface temperature of the weld seam was measured beneath the induction coil at the midpoint of the induction coil length.

Study Results

Welded test strips were inspected

visually, and were subjected to qualitative bend testing for evidence of cracking (longitudinal face-bend testing) and quantitative tensile testing. A total of 230 samples were tested. Selected samples were also subjected to a hardening (Q+T) cycle in an electrically heated box furnace prior to tensile testing. Specimens were heated to 1010°C, soaked for approximately 100 s, and air quenched. Subsequently, samples were given a low-temperature tempering treatment at 175°C for 30 min to simulate an electrocoating bake cycle.

Process Evaluation on Seam-Welded Tubing

The induction heating apparatus was implemented on a continuous roll-forming tube mill set up to produce 28.6 mm OD \times 0.5 mm wall and 19.1 mm OD \times 1.2 mm wall GTAW seam-welded 410 stainless steel tubing. Tubing was subjected to destructive mechanical testing to assess overall integrity and formability. Tubes were tested as-welded, with inductor cooling-control, and after a Q+T hardening cycle, for a total of 48 samples.

Guided Bend Weld Ductility

Figure 4 shows typical longitudinal face bend test samples after testing. Baseline control trials were run with no post-weld cooling control, and baseline process-annealed samples were run with a full-cooling to room tem-

Table 1 — Chemical composition (wt%) of Type 410 stainless steel used in study

Thickness, mm	C	Mn	S	P	Si	Cr	Ni	Al	Mo	N
0.5	0.14	0.41	0.003	0.024	0.30	11.75	0.12	0.002	0.02	0.01
1	0.14	0.37	0.003	0.032	0.40	12.25	0.24	0.001	0.03	0.01
2	0.12	0.45	0.003	0.025	0.34	12.55	0.50	0.001	0.04	0.01

Table 2 — Optimal induction heat-treatment parameters

Thickness, mm	Inductor power, %	Coil voltage, V	Coil amperage, A	Induction frequency, Hz	Net heat input to coil, kJ/mm	Average seam temp., °C
0.5	10	57	156	96	0.35	635
1	18	98	214	94	1.10	650
2	30	111	223	94	1.95	730

perature after welding followed by a seam annealing reheat pass. Samples were tested to failure (weld seam cracking) or until a complete U-bend was formed. Figures 5 and 6 show representative load-displacement test data. More specimens survived the bend test in the 4t configuration than the more-severe 2t setup. All baseline as-welded trials exhibited cracking prematurely. Conversely, all baseline process-annealed samples survived U-bend tests without cracking.

Two variables (downstream distance of the inductor coil and the induction power level) of the controlled-cooling trial parameters had the greatest effect on the bend-test performance. Ductility improved with moving the inductor downstream and increasing the power level to heat the seam sufficiently. Optimal ductility resulted with the inductor centerline ~30.5 cm downstream of the weld torch, and power level settings corresponding to average under-inductor seam temperature around 650°C.

Optimal Cooling-Control Parameters

Table 2 summarizes key induction heating parameters for optimal weld ductility improvement. For all thicknesses, the average cooling-control seam temperature underneath the induction coil was around 650°C; the upper critical (A_{C3}) for 410 stainless steel is about 960°C⁵. Tests performed at higher induction power settings,

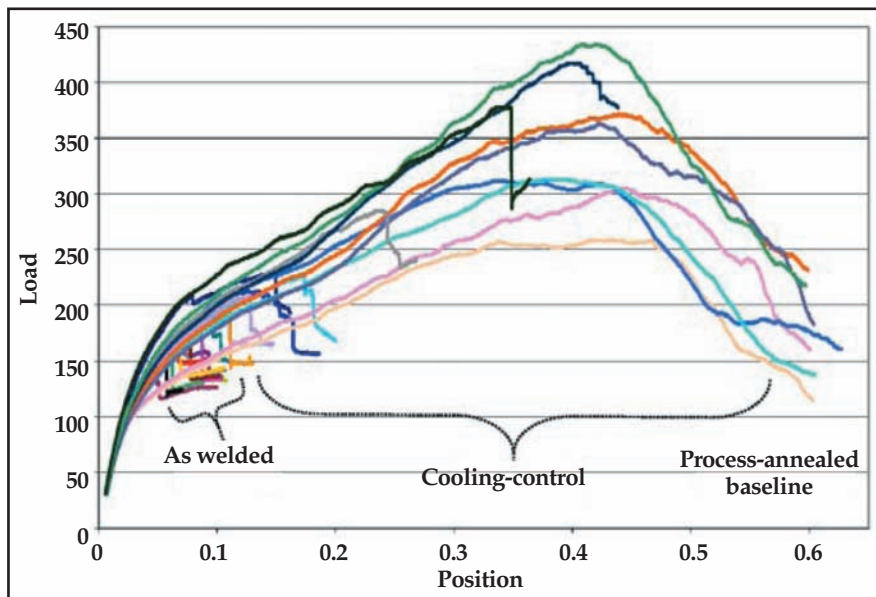


Fig. 6 — Comparison of 3-point longitudinal face-bend test load-position data for various process conditions. Modified ASTM E190 guided bend test for ductility of welds. Bend Radius = 4t; t = 1 mm.

and consequently, mean seam temperatures above A_{C3} , resulted in a decrease in ductility in the weld seam area. Conversely, tests performed at lower induction power settings, and lower mean seam temperatures, showed only slight increases in weld zone ductility.

For the 410 chemical composition used in this study, the predicted A_{C1} temperature is approximately 675°C, which agrees well with the experimental results; i.e., maximum softening occurs at inductor temperatures near the A_{C1} threshold, with increasing

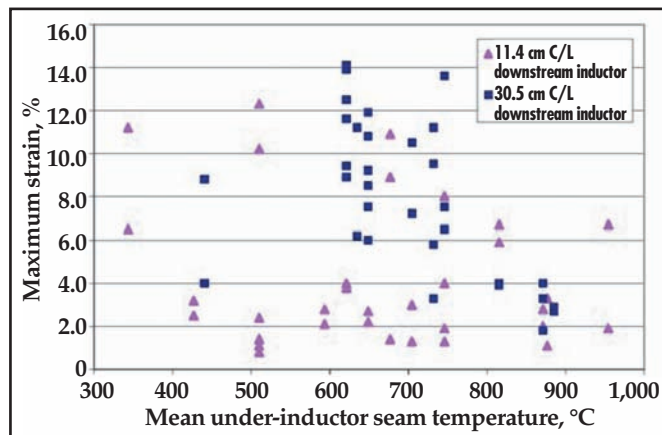


Fig. 7 — Maximum elongation versus mean under-inductor weld seam temperature for varying downstream inductor coil distances; longitudinal weld seam specimens include all gauges.

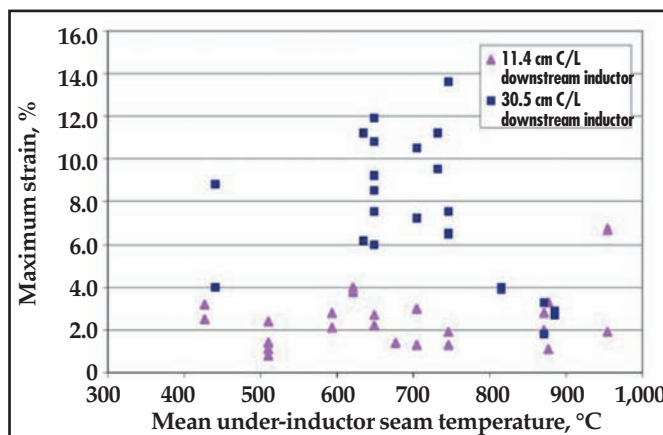


Fig. 8 — Maximum elongation vs. mean under-inductor weld seam temperature for varying downstream inductor coil distances; longitudinal weld seam specimens 1 and 2 mm only.

Martensitic Stainless Slashes Weight of Pickup Truck Tow Hook

With ever-increasing government regulations on vehicle safety and pressure from consumers concerned with fuel economy and emissions, car and truck manufacturers and their suppliers are turning to new technologies to help them achieve their goals of making components stronger and lighter. Much promise lies with advanced materials technologies using advanced engineering alloys or carbon composites. However, they have seen limited use in production due to high material costs and lack of compatibility with existing manufacturing processes.

Low cost martensitic stainless steels, on the other hand, provide excellent mechanical properties, including specific strength, toughness and fatigue performance, in addition to corrosion resistance while remaining easy to form, fabricate and process. Using martensitic stainless steels in place of other materials enables designers to arrive at cost-effective, lightweight structural solutions.

The development by KVA of a fully martensitic stainless steel full-size pickup truck front tow hook assembly illustrates these benefits. The assembly takes advantage of the excellent mechanical properties of hardened martensitic stainless to allow for notable weight savings—a 50% weight reduction compared with its high-strength, low-alloy (HSLA) counterpart. The use of seam-welded 410 stainless steel tubing in conjunction with a lower gauge stamped 410 stainless bracket exploit the material's ease of formability in the annealed state.

Benefits of the design include:

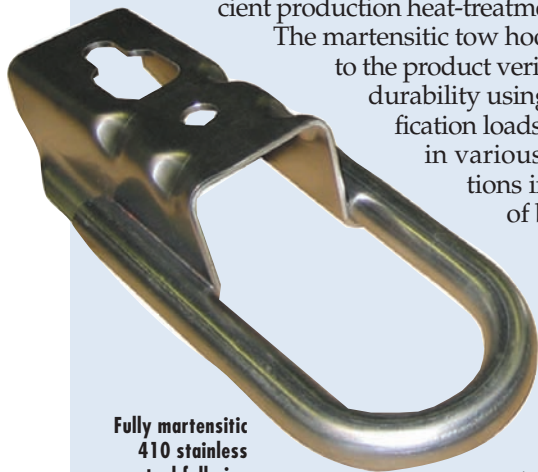
- Significant weight reduction (2.2 lb versus 4.4 lb)
- Surpasses current design strength requirement (no permanent set in severe loading cases)
- Unique brazed joint configuration
- Highly repeatable, economical, consistent bond assures product integrity with no loss of base metal mechanical properties due to weld HAZ degradation
- Additional corrosion protection from 410 stainless steel
- Low-force (i.e., low cost) production tooling needed to process soft, down-gauged sheet and tube

Bolt-On Implementation

GMAW welds of HSLA design are replaced with copper-brazed joints to affix the tow loop to the bracket. Brazing is accomplished during an air-quench bright-hardening cycle in a protective atmosphere. Excellent joint integrity and appearance, along with uniform hardness and tensile strength of 1,400 MPa throughout are obtained using the cost-effective, efficient production heat-treatment method.

The martensitic tow hook design was validated according to the product verification specifications for structural durability using static strength test criteria. Qualification loads of 125% of the GVW were applied in various pull orientations and configurations in tensile testing without any signs of breaking, bending, or other loss of function. Additional destructive tensile tests show the stainless steel design to have an additional 18% load capacity relative to the baseline HSLA part. This is due partly to a more even distribution of stress from the tow loop to the bracket on the stainless part's brazed configuration.

Conversely, the welds on the baseline HSLA part not only serve as stress concentrators (at the toe of the welds), but also they weaken the base metal in the heat affected zone.



Fully martensitic 410 stainless steel full-size pickup truck front tow-hook assembly.

hardness at higher inductor mean temperatures due to the rehardening of the weld seam.

Tensile Test Data

Figure 7 shows sample elongation data versus under-inductor mean weld seam temperatures for two downstream locations of the induction coil for all three test strip thicknesses. Although data from the induction coil immediately downstream of the welding torch (inductor centerline 11.4 cm downstream of weld torch) are scattered, samples with the induction coil further downstream (inductor centerline 30.5 cm downstream of weld torch) show a significant improvement in maximum weld-seam strain at failure. Greatest ductility benefits are obtained through induction heat-treatment near the A_{C1} temperature of 675°C.

The initial trial configuration, intended to slow the cooling rate of the weld seam in the 800-500°C range, with the inductor immediately downstream of the weld torch (11.4 cm inductor location), did not produce significant softening of the HAZ at any power levels. Some samples from this configuration actually showed a decrease in ductility compared with baseline welds. Much of the scatter in the 11.4 cm data set can be attributed to the 0.5 mm thickness tests, as the limited joint restraint on the 0.5 mm strips may account for the negligible effect of the cooling-control at any power level for that case. Figure 8 shows sample elongation versus temperature for the 1 and 2 mm thicknesses only. Figure 9 shows the necessary hold time to produce a mixed A+F+C (austenite + ferrite + chromium carbide) microstructure in type 410 MSS is about 200 s. The induction coil in the 11.4 cm location, even operating at the correct temperatures to catch the nose of the TTT curve, only holds the cooling weld seam near the proper temperature for approximately 10 s. Consequentially, with the inductor adjacent to the weld torch, the HAZ is never held at an intermediate temperature for sufficient time to promote the formation of the A+F+C microstructure directly from the molten weld pool.

Alternatively, with the inductor moved downstream from the weld torch, the weld pool has a chance to cool below the martensite start (M_s) temperature, approximately 330°C for type 410 stainless steel^[5]. The austenite

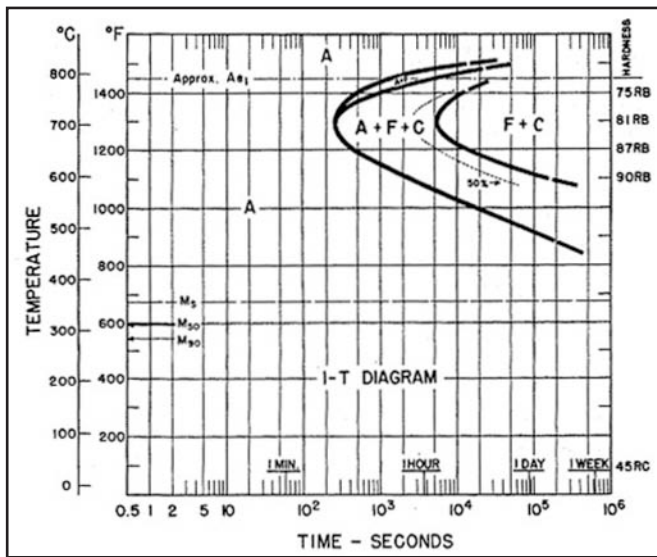


Fig. 9 — Time-temperature transformation (TTT) diagram for Type 410 stainless steel^[6].

in the weld seam is allowed to transform, at least partially, into martensite before being reheated by the inductor. This inductor cooling-control, equivalent to an air-quench tempering cycle, promotes transformation of the martensite into ferrite and very fine carbides. This transformation reduces strength, but it improves ductility and toughness^[5]. Additionally, the prolonged time at elevated temperatures increases diffusivity of hydrogen atoms while relieving thermal stresses, thereby reducing the probability of hydrogen-induced cracking or cold cracking^[5]. *Continued*



Fig. 10 — Typical tensile-test weld specimen fracture locations. From top: transverse (T), annealed base metal; longitudinal (L), annealed base metal; T, post-weld CC and Q+T; L, post-weld CC and Q+T.

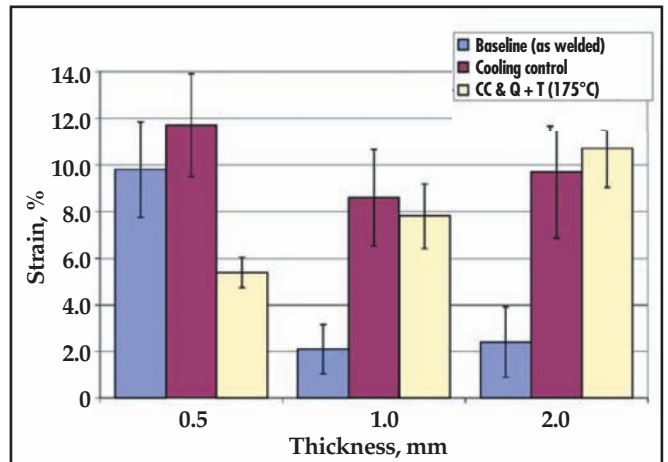


Fig. 11 — Comparison of maximum strain at fracture for optimum process conditions; DIN EN 895 longitudinal tensile specimen, average results for 62 trials.

ASM Heat Treating Society furnace donation fires enthusiasm for high school student.

How can we thank you enough for being so generous to our Materials Science and Engineering class here at Westerville South High School? This is definitely Christmas in April. All year, we've wished that we could have a furnace just like this one and now you have made our dreams come true!"

This is a story about an anonymous Founding Member of the ASM Heat Treating Society who saw an opportunity to reach out to young people with a message that "Materials are cool." Or its corollary that "Heat treating is hot!"

"We put your beautiful furnace to work immediately as our MSE class was working on their raku ceramics. All of the glazes we used contained various metal oxides which reduced to their metals on the surface of the clay."

A small heat treating furnace had been obtained to support the efforts of the ASM Materials Education Society and our Materials Camp and Teachers Camp programs in central Ohio. It was meant to be portable so that it could be lent out to teachers at different schools. But the furnace was too large to be moved and shipped cost effectively. It would have to remain in one place.

"With your furnace, we can also work with creating our own design with Nitinol, do a study of the solid phase changes for a Zn-Al alloy, and make our own glass."

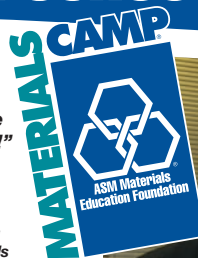
Rather than send the furnace back to its manufacturer, an HTS Founding Member had an idea. "I could write a check to cover the furnace and we would donate it to Westerville South High," he thought. "Then we could buy another smaller unit that could be used by teachers at other schools." A few phone calls were made, a check was sent and, almost immediately, the donated furnace was being used by eager students.

"We are the first Materials Science and Engineering class in central Ohio, and I plan on doing everything I can to help this to spread. Our first year has been highly successful and as a result, we have at least four students who want to pursue MSE in college."

Through this initiative, an individual member of our Heat Treating Society – the proud heat treating roots of ASM – stepped up to join with the ASM Materials Education Foundation "to excite young people in materials, science, and engineering careers."

"Thank you for helping us to inspire students to pursue Materials Science and Engineering as a career. And thank you again for your generosity and for valuing the education of our young people so highly!"

Very gratefully yours,
Elizabeth L. Eddy
 Westerville South High School Teacher



ASM Materials Education Foundation
www.asmfoundation.org

Fig. 12 — Comparison of ultimate tensile strength for optimum process conditions; DIN EN 895 longitudinal tensile specimen, average results for 62 trials.

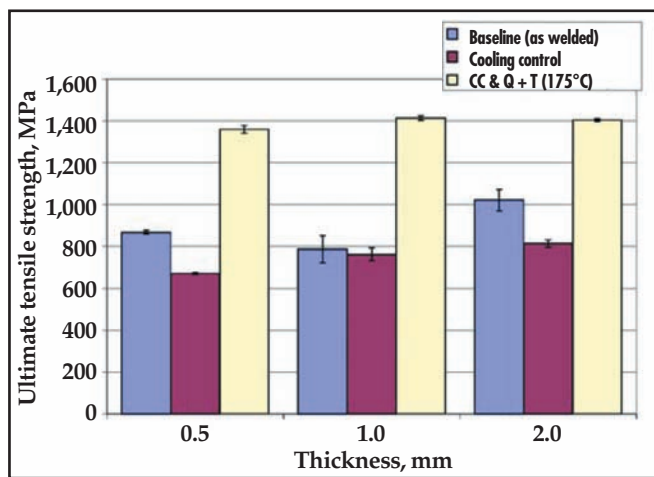


Fig. 13 — Tube mill weld-zone with inductor installed; material travel from left-to-right.

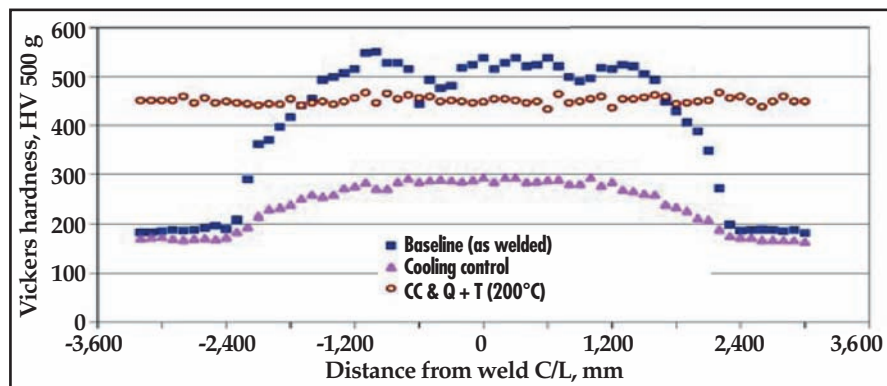


Fig. 14 — Typical Vickers microindentation hardness profile; load: 500 g; hardness spacing: 100µm; seam-welded 19.1 mm diameter × 1.2 mm Type 410 SS tubing.

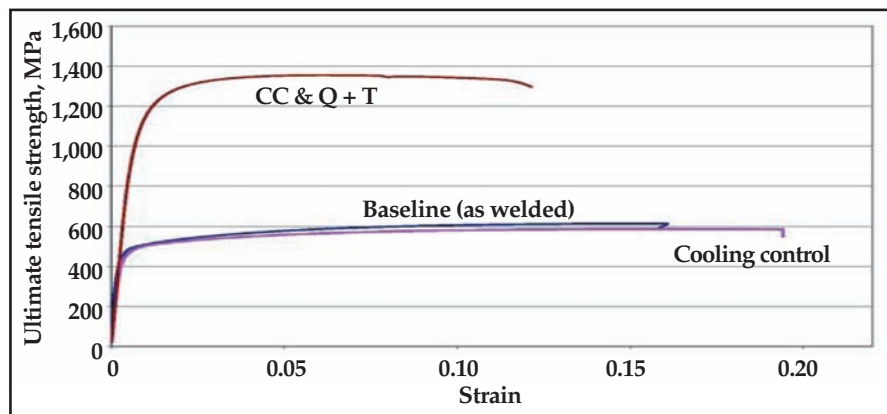


Fig. 15 — Typical stress-strain plots for seam-welded 28.6 mm diameter × 0.5 mm Type 410 SS tubing.

Figure 10 shows typical fracture locations in tensile test specimen. All transverse samples failed outside of the fusion and heat-affected zones for both the as-welded and heat-affected zones for both the as-welded/cooling-control, and the Q+T specimens. The as-welded/cooling control samples show significant necking in the fracture zone; this was expected with the annealed base metal properties. The as-welded/cooling-control longitudinal specimens typically exhibited brittle fracture in the fusion and HAZ regions, which caused the surrounding base metal to yield, but not fail until further loading. The Q+T hardened longitudinal specimens failed simultaneously across the fusion/HAZ/base metal interfaces, propagating along angles of maximum principal stress. Figures 11 and 12 show average results for longitudinal tensile testing of the baseline, optimal cooling-control, and Q+T weld specimens.

For all thicknesses, the optimum induction coil's cooling-control methods on the weld seam resulted in an increase in maximum strain at fracture and a corresponding decrease in ultimate tensile strength compared with the as-welded trials. The thicker gauges exhibit a better response to the controlled-cooling process; possibly due to the larger thermal inertia, and, therefore, slower effective cooling-rate after the inductor. The cooling-control weld specimens subjected to a Q+T thermal cycle exhibit strengths near 1,400 MPa, which is expected for hardened type 410 stainless steel.

Application to Seam-Welded Tubing

Following weld-strip testing, the cooling-control apparatus was installed on a seam-welded tube mill (Fig. 13). The inductor was placed approximately 30 cm downstream of the GTAW torch body, and power settings were adjusted to bring the under-inductor seam temperature to 550 to 650°C.

Typical microindentation hardness traverse data are shown in Fig. 14. The width of the HAZ in the as-welded sample is well over 3 mm. While not softened completely to the level of the base metal, the cooling-control significantly reduces the HAZ microindentation hardness relative to the as-welded sample. Furthermore, after a Q+T heat treatment, the microindentation hardness of the tube remains constant across the circumference, without any HAZ weakened areas.

Figures 15 and 16 show mechanical

properties at fracture. Similar to the butt-weld test strips, specimens run with inductor cooling-control show an increase in total axial elongation, with a corresponding slight decrease in ultimate tensile strength. The Q+T solution heat-treated samples show much less overall necking in the tube section, along with a markedly different angled fracture surface along the plane of maximum principal stress. Representative full-tube tensile specimens are shown in Fig. 17.

Figure 18 shows typical tube test specimens after flange testing. The HAZ-base metal interface crack is visible in the as-welded sample, whereas the controlled-cooling specimen is free of splits. The Q+T hardened samples exhibit splitting in the base metal, far away from the HAZ and weld zone.

The tubes were also subjected to hydroforming free-expansion burst testing (Fig. 19). All as-welded specimens show premature failure (splitting) in the weld/HAZ, unlike the cooling-controlled samples, which exhibit greater overall expansion and failures in the base metal.

Conclusions

Post-weld ductility of Type 410 MSS is improved by supplemental induction heating of the HAZ immediately following weld pool solidification. Applying optimum cooling-control methods on the weld seam results in an increase in maximum strain at fracture and a corresponding decrease in ultimate tensile strength compared with as-welded specimens. Improvements in ductility were more marked in thicker gauges. Strength levels, after a Q+T air-quench hardening cycle, were not affected by the cooling-control process. The as-welded HAZ microindentation hardness is reduced significantly with the addition of the cooling-control process. Applying optimal cooling-control parameters to a seam-welded tube mill increases formability of MSS tubing. **HTP**

References

1. C.L. Tsai and C.M. Tso, ASM Handbook, Vol. 6, 10th Ed., *Welding, Brazing and Soldering*, ASM Intl., Matls. Park, Ohio, 1993.
2. N.M. Watson, Laser welding of structural steel with wire feed, The Welding Institute, UK, 1985.
3. C. Bagger, et.al., Induction heat treatment of laser welds, *J. of Laser Appl.*, Vol. 15, No. 4, Laser Inst. of Am., Fla., 2003.
4. S.L. Semiatin and D.E. Stutz, *Induction Heat Treatment of Steel*, ASM Intl., Matls. Park, Ohio, 1986.

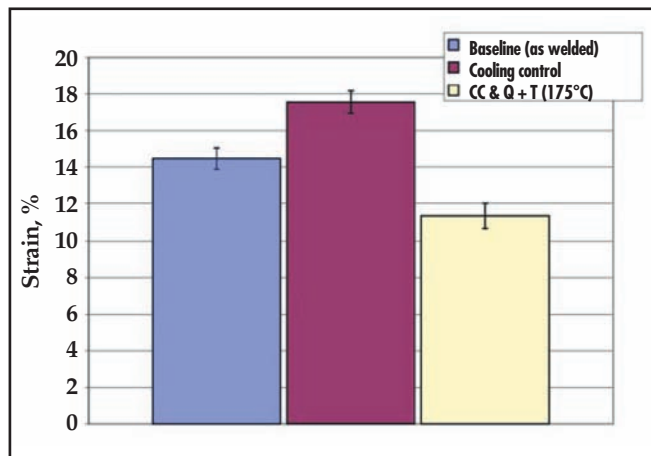


Fig. 16 — Comparison of maximum strains at fracture for seam-welded 28.6 mm diameter x 0.5 mm Type 410 SS tubing, average results for 16 trials.

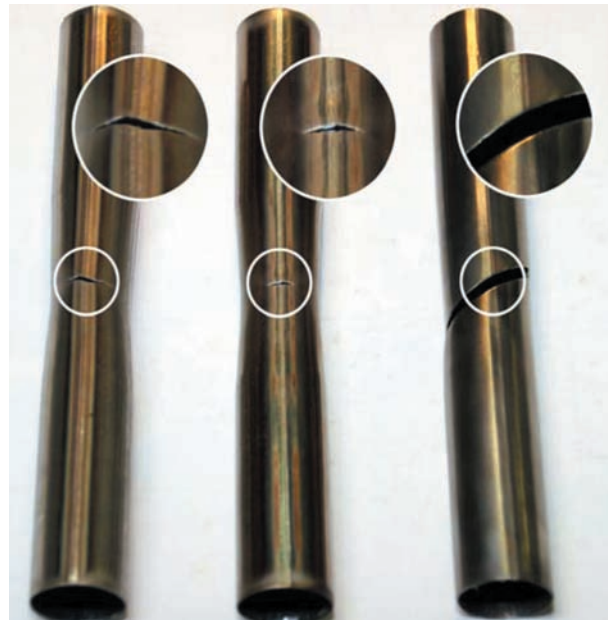


Fig. 17 — Typical tensile test tube specimens; from left: as welded; cooling-controlled; C.C. Q+T hardened.



Fig. 18 — Typical ASTM A513 ring flare-test tube specimens; from left: as welded; cooling-controlled; CC Q+T hardened.



Fig. 19 — Typical hydroformed free expansion burst test specimens; (top) as welded; (bottom) cooling-controlled.

5. J.C. Lippold and D.J. Kotecki, *Welding Metallurgy and Weldability of Stainless Steels*, John Wiley & Sons, N.J., 2005.
6. E. McCrink, Seam-Welded Air Hardenable Steel Constructions, U.S. Pat. 7,232,053, KVA Inc., 2007.

For more information: Daniel Codd, principal mechanical engineer, KVA Inc., 124 South Market Place, Ste. 200, Escondido, CA 92029-1303, tel: 760-489-5821; e-mail: dcodd@kvastainless.com; Web site: www.kvastainless.com.